On the temperature behavior of shunt-leakage currents in Cu(In,Ga)Se2 solar cells: The role of grain boundaries and rear Schottky contact

On the temperature behavior of shunt-leakage currents in $Cu(In,Ga)Se_2$ solar cells: the role of grain boundaries and rear Schottky contact

G. Sozzi[1], R. Menozzi[1], N. Cavallari[2], M. Bronzoni[2], F. Annoni[2], M. Calicchio[2], M. Mazzer[2]
[1] Department of Information Engineering - University of Parma
Parco Area delle Scienze 181A, 43124 Parma, Italy
[2] IMEM-CNR Institute, Parco Area delle Scienze 37A, 43124 Parma, Italy

ABSTRACT — **By comparing simulated and measured dark current-voltage (I-V) characteristics of CIGS cells at different temperatures, we investigate the temperature behavior of the shunt leakage current, and find that it can be explained by large donor trap concentrations at grain boundaries (GBs), and by a Schottky barrier at the backside contact where the GBs meets the anode metallization. We studied the I-V characteristics in the temperature range 280 K - 160 K achieving good fits of the measured I-V curves, especially for reverse bias and low forward bias, where the shunt leakage current dominates. The most important parameters determining the shunt leakage current value and its temperature dependence are the peak energy and density of the GB donor distribution, which control the inversion of GBs and the pinning of Fermi level at the anode/GB contact.**

Index Terms **— shunt-leakage current, grain-boundary, Schottky contact, thin-film photovoltaics, CIGS.**

I. INTRODUCTION

Thin-film photovoltaic technologies, and CIGS cells in particular, are important alternatives to crystalline silicon solar cells, because they combine cost effective preparation methods with conversion efficiencies up to 21.7 %. Although understanding the cell properties and the conduction mechanisms that control its behavior is essential to obtain further efficiency improvements, not even the dark current-voltage (I-V) characteristic is fully understood yet. One key issue affecting the cell performance is the excess of dark leakage current at low bias, commonly known as shunt leakage current, which degrades the cell performance [1]. In fact, solar cells based on poly-crystalline chalcopyrite absorbers often show I-V characteristics that deviate from the exponential behavior of the classical theory: recombination currents are many orders of magnitude larger than expected and often characterized by ideality factor $n > 2$ at low voltage (high-voltage $n > 2$ is typically due to series resistance) [2]. Tunneling-enhanced recombination can explain ideality factors > 2 only at low temperature (< 200 K) [3] or for devices with high doping, while it is seldom important for temperatures approaching 300 K.

By using 2D numerical simulations, we recently explained the observed anomalous (> 2) ideality factor by large donor trap concentrations at grain boundaries, and SRH recombination therein, with no need of complex models involving tunneling, coupled traps or interface recombination [4].

We now turn to analyzing the temperature dependence of the dark current of CIGS cells, again with the aid of 2D numerical simulations. As explained above, tunneling can account for the increase of current magnitude at low voltage, but only in the case of highly doped junctions [5]. Moreover, the shunt leakage current has weak temperature dependence, symmetry around $V = 0$ and non-linear voltage dependence, i.e., non-ohmic shunt behavior [2]. A power law dependence of current on voltage, as in the space-charge limited current (SCLC) model, captures all these aspects, but only assuming the presence of intrinsic regions inside the p-doped CIGS [2], which is not the case here.

We study the origin of shunt leakage currents without resorting to tunneling or SCLC. We start from experimental dark I-V curves of CIGS cells measured over a 120 K range and investigate the current conduction using numerical simulations. We show that, assuming high concentration of donor traps at grain boundaries and a Schottky contact at the anode/GB contact, we can model the behavior of the measured I-V curves over a wide temperature range.

II. METHODS

A. Samples, Measurements and Observations

The CIGS-based solar cell we consider has 15.25% efficiency and consists of a soda-lime glass substrate, 500 nm thick Mo back contact, 1 μm-thick CIGS absorber, 120 nm CdS buffer, and 820 nm Al-doped ZnO window layer; it was fabricated using a low-temperature single-stage production process based on pulsed electron deposition (PED) [6]. The experimental dark I-V curves measured at temperatures of 280 K, 260 K, 220 K, 180 K and 160 K are shown in Fig.1; the existence of three distinct regions in the I-V curves (regions I, II, and III) is marked in Fig. 1. While the current in region III follows the theoretical exponential behavior and flattens out at high voltage due to series resistance, regions I and II are dominated by the shunt leakage current, which exceeds the classical diode current by several orders of magnitude. The voltage corresponding to the onset of region III decreases with temperature. The shunt current (I and II) is symmetrical with respect to $V = 0$ V and weakly temperature-dependent, with the current decreasing by a factor of 15 over a 120 K range. The ideality factors in region I and II have values well above 2 for all temperatures.

B. Simulations

We simulated the poly-crystalline CIGS cells using the Synopsys Sentaurus-Tcad suite [7]. The cell behavior in the dark is described by the Poisson, electron and hole continuity, and drift-diffusion equations; recombination via deep defects follows the SRH model as detailed in [8], [9]. For simplicity, we assume grains with uniform size, of width g = 0.75 μm.

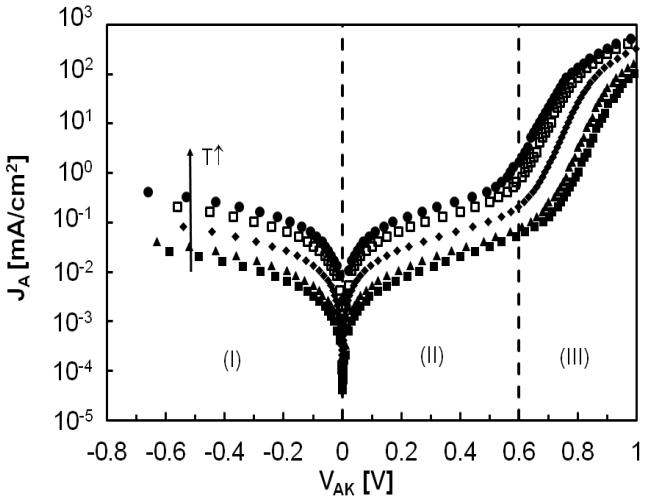

Fig. 1. Experimental dark I-V characteristics at 280, 260, 220, 180, and 160 K. Regions I and II are dominated by the shunt leakage current, while region III is dominated by the classical diode current.

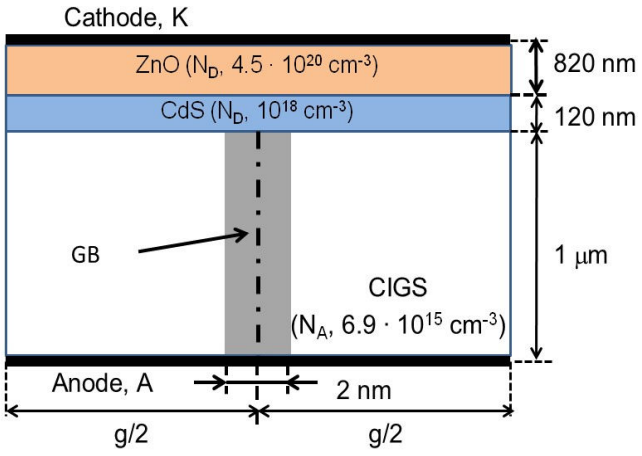

Fig. 2. The simulated solar cell (not to scale). g = 0.75 μm. The 2 nm-wide gray shaded region models the GB.

The grain boundary (GB) is modeled as a thin (2 nm) layer (Fig. 2) decorated by donor traps with a Gaussian energy distribution, the critical parameters of which are (i) the peak concentration N_{DT}^{PEAK}, (ii) the peak energy E_T and (iii) the standard deviation w_T. Deep traps are also in the grain interior (GI). A full description of simulation parameters are given in Table I, while the choice of GB parameters is described below. The anode and cathode contacts are ohmic; however, in order to reproduce the measured curves over temperature, we introduce a non-linear lumped resistance where the GB meets the anode contact simulating the presence of a Schottky barrier [10], as detailed below. Finally, in order to fit the measured I-V curves at high voltage (V_{AK} > 0.7 V at 280 K), a parasitic resistance of 0.4 Ω·cm^2 is placed in series with the cathode.

TABLE I
MATERIAL PARAMETERS USED IN THE SIMULATIONS AT 280 K

Material	ZnO	CdS	CIGS
Eg [eV]	3.3	2.4	1.15
Doping [cm^{-3}]	$4.5\cdot10^{20}$ (acceptor)	10^{18} (acceptor)	$6.9\cdot10^{15}$ (donor)
$\varepsilon/\varepsilon_0$	9	10	13.6
m_e/m_0	0.2	0.2	0.09
m_h/m_0	1.2	0.8	0.72
χ [eV]	4.5	4.3	4.6
μ_e [cm^2/(V·s)]	100	100	90
μ_h [cm^2/(V·s)]	25	25	12.5
Bulk Trap Density [cm^{-3}]	10^{16} (donor)	10^{16} (donor)	10^{15} (donor)
Bulk Trap Energy [eV]	midgap	midgap	midgap
Bulk Trap capture cross sections [cm^2]	σ_e : 10^{-16} σ_h : 10^{-13}	σ_e : 10^{-15} σ_h : 10^{-12}	σ_e : $2\cdot10^{-14}$ σ_h : $1\cdot10^{-15}$

III. RESULTS AND DISCUSSION

Starting from the results of [4], we tried to simulate the temperature behavior of the I-V curves by decorating the GB with a Gaussian energy distribution of donor defects.

In the presence of sufficiently high concentration of ionized donor traps inside it, the GB becomes inverted and electrons starts flowing through the cell along the GB, giving rise to huge simulated shunt leakage currents, as shown in Fig. 3.

The choice of N_{DT}^{PEAK}, E_T and w_T determines the magnitude and voltage and temperature dependence of the shunt leakage current. By comparing simulations performed for different combinations of these parameters, we found that E_T is the most important parameter to reproduce the I-V curve over temperature: as E_T is lowered from the conduction band minimum Ec and approaches the midgap, the ionized donor concentration in the GB drops at lower temperatures, with the effect of reducing the inversion of the GB and inhibiting the electron conduction therein. Thus, the shunt leakage current is large at higher temperatures, but rapidly disappears for low

temperatures, unlike in the real cell. Thus, in order to simulate the presence of shunt currents at the lowest temperatures, E_T must be close to Ec. w_T also affects the reduction of ionized donor concentration with temperature and controls the shape of the I-V curve, while N_{DT}^{PEAK} determines the maximum donor concentration, which ultimately limits the GB inversion. In Fig. 3 we show the simulated I-V curves obtained with the following set of parameters: $N_{DT}^{PEAK} = 3 \cdot 10^{19}$ $eV^{-1} \cdot cm^{-3}$, $E_T - E_V = 0.9$ eV, $w_T = 0.12$ eV, and capture cross sections $\sigma_{e/h} = 2 \cdot 10^{-17}$ cm^2. We can reproduce the I-V symmetry around V = 0 V, but the currents are too large, and their temperature dependence too strong (the simulated current decreases by a factor of ~ 900 over the 120 K range) in regions I and II, to the point of obscuring the diode-dominated region III.

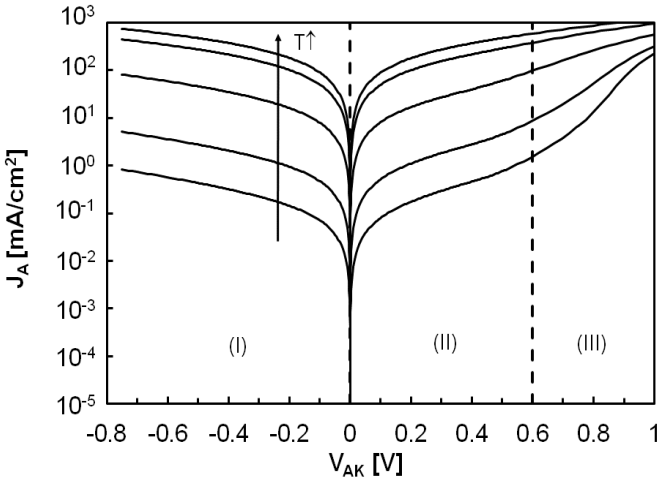

Fig. 3. Simulated current density versus anode to cathode voltage at 280, 260, 220, 180, and 160 K.

In order to gain better insight of the temperature behavior of measured I-V curves, we extracted the resistance Rc for V_{AK} approaching 0 V from the measured data of Fig. 1; the values are in the inset of Fig. 4. As shown in Fig. 4, the measured data are modeled reasonably well by a Schottky diode model, whereby [10]:

$$Rc = k/(qA^*T) \cdot \exp(q\phi_B/kT) \qquad (1)$$

The extracted $q\phi_B = 0.0716$ eV is low if compared with other measured values [11], suggesting the pinning of Fermi level due to the high concentration of donor traps inside the GB, i.e., a Schottky barrier near to the Bardeen limit [12]. We thus inserted this temperature-dependent series resistance R_C at the anode/inverted-GB portion of the anode/CIGS junction, with the rest of the anode contact behaving as a standard ohmic contact. By inserting the measured values of Rc in series with the anode/GB contact, we simulated the I-V curves of Fig. 5, which show that Rc allows to obtain excellent fit of the characteristics in region I, where the GB dominates all over the 120 K range. In region II, the fitting is good up to about $V_{AK} = 0.3$ V, after which the characteristics tend to be lower than the measured ones, the match worsening at lower temperature. The reason for the mismatch at higher bias is that the R_C we inserted is the one extracted from the measurements for V_{AK} approaching 0 V, which overestimates the resistance of the Schottky contact at forward bias. In fact, the Schottky barrier height at the GB/anode interface depends on the ionized defect density, which is reduced by forward bias.

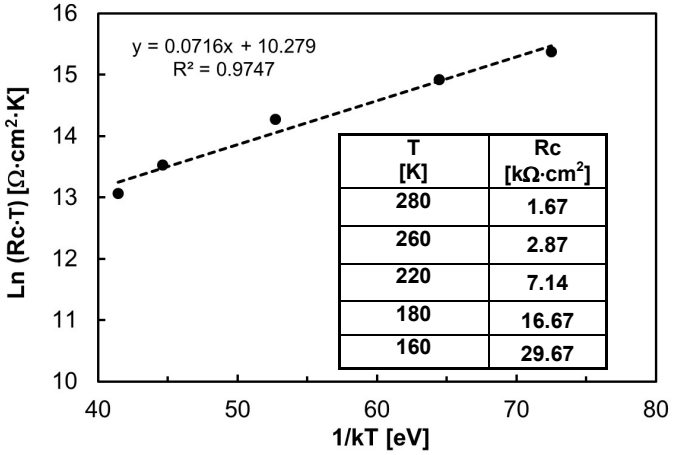

Fig. 4. Extracted values of the equivalent Schottky resistance and corresponding interpolation curve.

Unfortunately, the simulator does not allow inserting such a Schottky contact boundary condition, which should correspond to an equivalent Schottky resistance the value of which is reduced by forward bias.

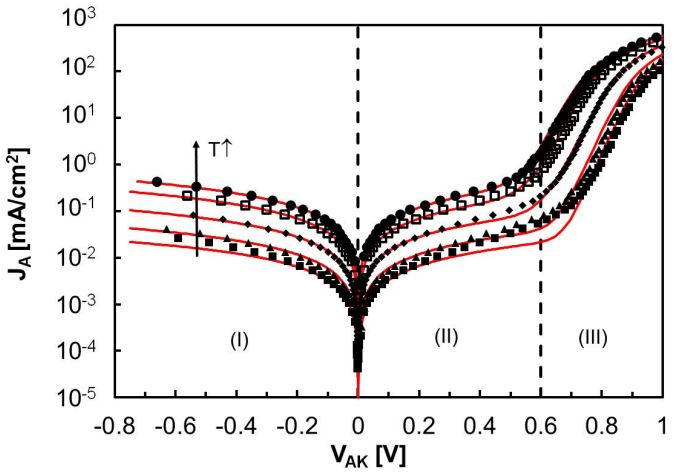

Fig. 5. Measured (symbols) and simulated (lines) current density versus anode to cathode voltage at 280, 260, 220, 180, and 160 K.

As a consequence, when the cell is forward biased, the ohmic drop across Rc is too large, the GB potential increase is too low, therefore: (i) the GB is less attractive to electrons coming from the cathode, and (ii) the GI remains depleted of holes: this is the reason why the simulated current in region II and at the onset of region III is lower than the measured one for $V_{AK} > 0.2$ V. The effect is smaller for higher temperature because the depletion of the GI is less severe.

Again, the fitting of measured data in region III is better for the highest temperatures. An additional source of mismatch with measurements may also be the electron and hole lifetimes in the GI changing with temperature. We obtained the simulated curves of Fig. 5 assuming a hole capture cross section in the GI with an Arrhenius temperature dependence [13] ($\sigma_h = 1 \cdot 10^{-15}$ cm^2 at 280 K and $2 \cdot 10^{-12}$ cm^2 at 160 K).

VI. Conclusion

We used 2D simulations to investigate the temperature behavior of measured shunt leakage current of CIGS cells in the 160-280 K range, explaining it as originating from large donor trap concentrations at grain boundaries (GBs), and by a Schottky barrier at the rear contact where the GBs meets the anode metallization. We obtained good fit of the I-V characteristics. The most important parameters determining the shunt leakage current and its temperature dependence are the peak energy and density of the GB donor distribution, which control the inversion of GB and the pinning of Fermi level at the anode/GB contact.

References

[1] A. Virtuani, E. Lotter, M. Powalla, U. Rau, J. H. Werner, and M. Acciarri, "Influence of Cu content on electronic transport and shunting behavior of Cu (In,Ga)Se2 solar cells", *Journal of Applied Physics*, vol. 99, 014906, 2006.

[2] S. Dongaonkar, J. D. Servaites, G. M. Ford, S. Loser, J. Moore, R. M. Gelfand, H. Mohseni, H. W. Hillhouse, R.Agrawal, M. A. Ratner, T. J. Marks, M. S. Lundstrom, and M. A. Alam, "Universality of non-Ohmic shunt leakage in thin-film solar cells", *Journal of Applied Physics*, vol. 108, pp. 124509 , 2010.

[3] U. Rau, and H. W. Schock, "Electronic properties of Cu(In,Ga)Se_2 heterojunction solar cells–recent achievements, current understanding, and future challenges", *Applied Physics A*, vol. 69, pp. 131–147, 1999.

[4] G. Sozzi, R. Mosca, M. Calicchio, and R. Menozzi, "Anomalous dark current ideality factor (n > 2) in thin-film solar cells: the role of grain-boundary defects", *40th IEEE Photovoltaic Specialist Conference (PVSC)*, pp.1718-1721, 2014.

[5] G. A. M. Hurkx, D. B. M. Klaassen, M. P. G. Knuvers, "A New Recombination Model for Device Simulation Including Tunneling", *IEEE Transactions on Electron Devices*, vol. 39, pp. 331-338, 1992.

[6] S. Rampino, F. Annoni, M. Bronzoni, M. Calicchio, E. Gombia, M. Mazzer, F. Pattini, and E. Gilioli, "Joule heating-assisted growth of Cu(In,Ga)Se2 solar cells"**,** *Journal of Renewable and Sustainable Energy*, vol. 7, 013112, 2015.

[7] http://www.synopsys.com/Tools/TCAD

[8] G. Sozzi, F. Troni, R. Menozzi, "Numerical analysis of the effect of grain size and defects on the performance of CIGS solar cells", in *Proc. CS-MANTECH*, 2010, pp. 353-356.

[9] G. Sozzi , F. Troni, R. Menozzi, "On the combined effects of window/buffer and buffer/absorber conduction-band offsets, buffer thickness and doping on thin-film solar cell performance", *Solar Energy Materials & Solar Cells*, vol. 121, pp. 126–136, 2014.

[10] K. Varahramyan and E. J. Verret, "A model for specific contact resistance applicable for titanium silicide-silicon contacts", *Solid-State Electronics*, vol. 39, pp. 1601-1607, 1996.

[11] E. Schlenker, V. Mertens, J. Parisi, R. Reineke-Koch, M. Köntges, "Schottky contact analysis of photovoltaic chalcopyrite thin film absorbers", *Physics Letters A,* vol. 362, pp. 229–233, 2007.

[12] E. H. Rhoderick and R. H. Williams, "*Metal-Semiconductor Contacts*", Clarendon Press, Oxford, 1988.

[13] P. Blood and J. W. Orton, "*The Electrical Characterization of Semiconductor: Majority Carriers and Electron States*", Academic Press, London, 1992.